

HiMu: Hierarchical Multimodal Frame Selection for Long Video Question Answering

Dan Ben-Ami¹ Gabriele Serussi¹ Kobi Cohen² Chaim Baskin¹

¹INSIGHT Lab, Ben-Gurion University of the Negev, Israel

²Ben-Gurion University of the Negev, Israel

Abstract

Long-form video question answering requires reasoning over extended temporal contexts, making frame selection critical for large vision-language models (LVLMs) bound by finite context windows. Existing methods face a sharp trade-off: similarity-based selectors are fast but collapse compositional queries into a single dense vector, losing sub-event ordering and cross-modal bindings; agent-based methods recover this structure through iterative LVLM inference, but at prohibitive cost. We introduce HiMu, a training-free framework that bridges this gap. A single text-only LLM call decomposes the query into a hierarchical logic tree whose leaves are atomic predicates, each routed to a lightweight expert spanning vision (CLIP, open-vocabulary detection, OCR) and audio (ASR, CLAP). The resulting signals are normalized, temporally smoothed to align different modalities, and composed bottom-up through fuzzy-logic operators that enforce temporal sequencing and adjacency, producing a continuous satisfaction curve. Evaluations on Video-MME, LongVideoBench and HERBench-Lite show that HiMu advances the efficiency–accuracy Pareto front: at 16 frames with Qwen3-VL 8B it outperforms all competing selectors, and with GPT-4o it surpasses agentic systems operating at 32–512 frames while requiring roughly 10× fewer FLOPs.

Keywords: Video Question Answering Frame Selection Neuro-Symbolic Reasoning Multimodal Understanding

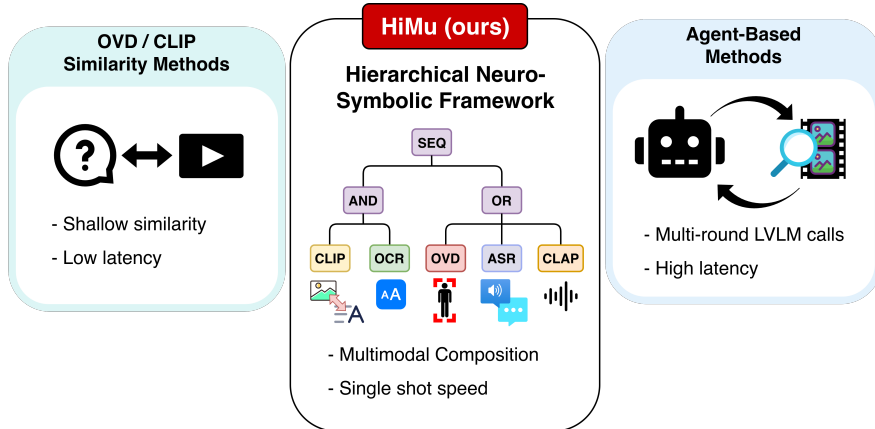


Figure 1: **Three paradigms for query-aware frame selection.** **Left:** Similarity methods use global embeddings, offering low latency but lacking compositional reasoning. **Right:** Agentic methods achieve deep understanding via iterative LVLM calls at prohibitive cost. **Center:** HiMu (ours) decomposes queries into logic trees evaluated by lightweight experts, achieving multimodal compositional selection at single-shot speed.

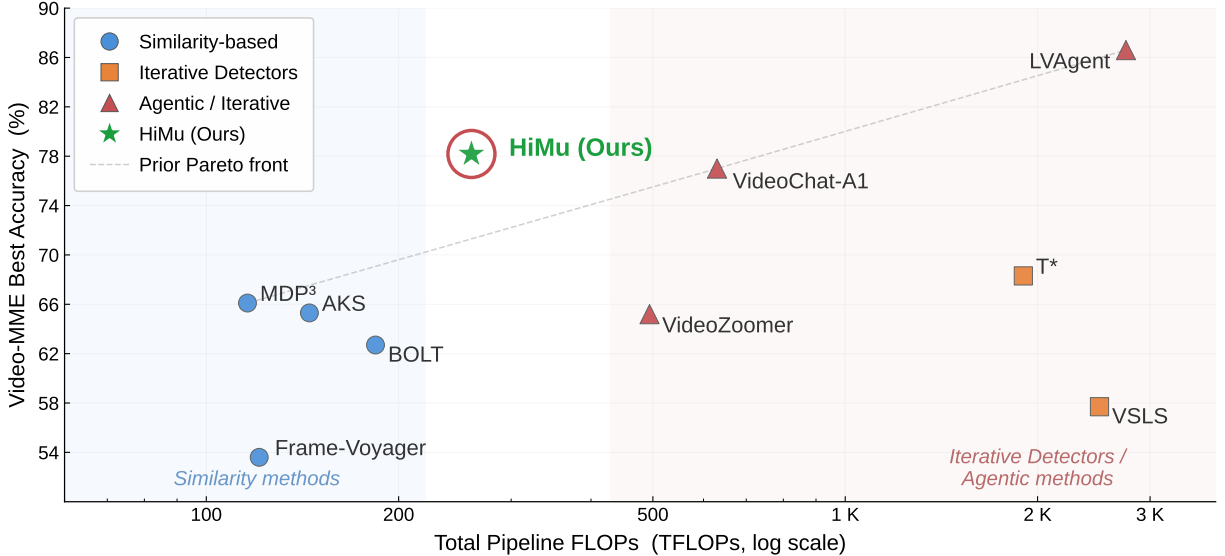


Figure 2: **Accuracy vs. computational cost of frame selection methods.** Top-reported accuracy on Video-MME versus total pipeline FLOPs (TFLOPs, log scale) for a 10-minute video on 8×A100 GPUs. Similarity-based selectors (blue) are computationally efficient but plateau at low accuracy; agentic and iterative detector based methods (red region) reach higher accuracy at a substantially greater cost; and HiMu (ours, green star) breaks the prior Pareto front.

1 Introduction

Long-form video question answering (VideoQA) requires reasoning over extended temporal horizons. Due to the finite context windows of current large vision-language models (LVLMs) [1, 2, 3], processing entire videos at native frame rates is computationally infeasible. Consequently, frame selection becomes a critical bottleneck: a model, regardless of its expressiveness, can only answer correctly if it is provided with the relevant visual evidence.

Existing frame selection strategies face a sharp trade-off between efficiency and reasoning depth (Fig 2, Fig 1, Left and Right). Similarity-based approaches typically score frames against the query using a frozen vision-language encoder [4, 5, 6, 7, 8]. While computationally lightweight, these methods collapse long and compositional queries into a single dense vector, forcing distinct temporal and semantic constraints to be evaluated through a single global similarity score. For instance, answering “*After the narrator mentions the chemical reaction, what happens to the beaker on the left?*” inherently requires reasoning across both the audio track (the narration) and the visual track (the beaker’s state). By definition, a single-modality vision-language encoder is blind to auditory events, making it fundamentally impossible to capture such cross-modal temporal dependencies within a monolithic similarity score.

Conversely, agent-based methods [9, 10, 11, 12] and per-frame scoring techniques [13, 14] achieve compositional understanding through iterative search and multi-round LVLm inference. However, this accuracy comes at a prohibitive computational cost, often incurring latencies 10-100× higher than similarity-based selectors (Table 1). This dichotomy suggests that sophisticated compositional reasoning is intrinsically linked to expensive iterative inference.

We challenge this assumption with **HiMu** (**H**ierarchical **M**ultimodal **F**rame **S**election), a framework demonstrating that compositional structure can be resolved efficiently prior to any LVLm

evaluation (Fig 1, center). The core insight is that complex natural language queries inherently decompose into structured logical trees. HiMu leverages a single, text-only LLM call to parse the input query into a hierarchical tree of atomic predicates. Each leaf node is routed to a lightweight, modality-specific expert. These localized signals are then evaluated over the video timeline and composed bottom-up using continuous fuzzy-logic operators, yielding a per-frame *satisfaction curve* $T(t) \in [0, 1]$.

HiMu is a training-free framework and can be seamlessly integrated as a plug-and-play module for any LVLM. By caching expert features per video, the per-query overhead is reduced to a lightweight tree evaluation and subsequent signal post-processing, entirely eliminating the need for iterative visual token processing during selection. Consequently, as shown in Fig. 2, HiMu redefines the efficiency-accuracy Pareto front on Video-MME [15]. It achieves 78.18% accuracy, getting closer to the performance of state-of-the-art agentic models [11] while requiring approximately $10\times$ fewer FLOPs, and consistently outperforms similarity-based selectors with only a modest increase in computational cost.

Our **contributions** can be summarized as follows:

- A **neuro-symbolic framework** that decomposes video queries into hierarchical logic trees, routing atomic predicates to modality-specific experts and composing their signals via **fuzzy-logic operators** for precise temporal grounding.
- A **training-free, single-shot pipeline** that replaces iterative LVLM calls with a single text-only LLM planning step and cached expert evaluation, yielding negligible per-query latency.
- A **redefined efficiency-accuracy Pareto front** on Video-MME [15], LongVideoBench [16], and HERBench [17], demonstrating that HiMu comprehensively bridges the gap between fast similarity methods and expensive agentic approaches under constrained frame budgets.

2 Related Work

Frame selection methods for long-video QA span a spectrum from fast but shallow similarity scoring to accurate but expensive multi-call reasoning. We organize prior work along this efficiency–reasoning axis, and separately review token-compression methods that address a complementary bottleneck.

Similarity-based frame selection. The most efficient selectors score each frame against the query through a frozen vision-language encoder. BOLT [6] pairs query-frame similarity (e.g., CLIP [4]/ SigLIP [5]) with inverse-transform sampling to prioritize relevant frames while preserving selection diversity; AKS [7] recursively splits the timeline, allocating more keyframes to high-scoring segments; and MDP³ [8] formulates selection as a determinantal point process solved via dynamic programming, capturing relevance, diversity, and sequentiality. These methods add minimal overhead, yet they collapse multi-clause queries into a single dense representation, offering limited capacity to preserve sub-event ordering or cross-modal bindings—e.g., a query like “*What does the chef add right after mentioning the secret spice?*” requires distinguishing a spoken reference from a visual action *and* enforcing their temporal adjacency, which can be largely lost in a single embedding. Learning-based variants (e.g. Frame-Voyager [18], FFS [19], MLLM-FS [20], VidF4 [21]) train scoring or policy modules for richer signals, but require task-specific supervision. Most selectors in this family compute scores from visual-only features; audio, when available, is typically consumed downstream rather than used to drive selection.

Structured and logic-based selection. A second line of work injects explicit relational or logical operators into selection. T* [22] (detector-based variant) casts temporal search as spatial search, using YOLO-World [23] to iteratively zoom into relevant frames; VSLS [24] defines four logical dependencies (spatial co-occurrence, temporal proximity, attribute dependency, causal order) and iteratively refines sampling; and NeuS-QA [25] translates queries into a temporal-logic specification and constructs a video automaton by scoring atomic propositions at the frame level with a VLM, which can be costly on long videos due to dense proposition grounding. These are meaningful steps toward compositional reasoning, yet VSLS uses four predefined relations rather than a general nested temporal-logic language, limiting expressivity for interleaved constraints (*e.g.* $(A \text{ after } B) \text{ AND } (C \text{ during } A)$); T* performs iterative zooming but does not offer a general compositional program over sub-events; and NeuS-QA’s dense grounding cost can approach that of multi-call methods. HiMu instead supports nested structure via a hierarchical tree and grounds leaves through cached lightweight experts (*e.g.*, ASR, CLAP [26], object detector), avoiding LVLM calls during selection.

Multi-call reasoning. Multi-call systems trade compute for depth, either through LLM-agent planners that iteratively call tools, or LVLM-in-the-loop selectors that repeatedly score within the selection loop. VideoAgent [9] constructs a structured unified memory with tool calls for segment localization; LVAgent [11] coordinates MLLMs through multi-round discussion; LongVideoAgent [12] trains a master LLM with reinforcement learning for multi-step evidence gathering; and VideoTree [27] builds a query-adaptive segment tree via coarse-to-fine keyframe extraction. VideoZoomer [28] performs multi-turn temporal zooming via iterative tool calling, and SeViLA [13] and A.I.R. [14] invoke a strong VLM within the selection loop for localization and iterative refinement, at substantially higher cost (Table 1). These approaches fundamentally couple compositional reasoning to iterative LVLM inference.

Token compression and pruning. Orthogonal to frame selection, token-reduction methods decrease visual tokens *per frame*: LongVU [29] applies spatiotemporal compression, while FastV [30] prunes redundant tokens in intermediate LLM layers. These are complementary - they decide *how many tokens* each frame contributes, whereas HiMu decides *which frames* to include - and can in principle be combined to extend the effective frame budget under the same context length.

The analysis above reveals a gap: efficient methods lack compositional structure, while compositional methods require expensive multi-call inference. HiMu addresses this gap by factoring compositional reasoning into a one-shot text-only LLM planning step and a bank of cached lightweight experts, enabling structured selection without LVLM calls during selection. Audio is comparatively underexplored as explicit selection evidence in query-aware long-video QA pipelines, which rely primarily on visual-text cues; HiMu incorporates non-speech audio via audio-text alignment signals (CLAP [26]) as a first-class selection modality. Table 1 summarizes these distinctions.

3 Method

Given a video $\mathcal{V} = \{v_1, \dots, v_T\}$ sampled at a fixed rate (*e.g.* 1 fps) with its audio track, a natural-language question Q (optionally with answer options), and a frame budget K , HiMu selects the K most question-relevant frames for a single downstream LVLM call. The pipeline (Fig. 3) proceeds in four stages: (i) a text-only LLM decomposes Q into a hierarchical logic tree \mathcal{T} (Sec. 3.1); (ii) each leaf is scored by a modality-specific expert, and the resulting signals are lightly post-processed (Sec. 3.2); (iii) signals are composed bottom-up via fuzzy-logic operators into a per-frame

Table 1: Comparison of frame selection methods for long-form video QA. **Selector latency** excludes the final QA call. Latency is estimated for a 10-minute video (600 frames at 1 FPS, $K=16$) on $8\times A100$ (80 GB). **E2E** is first-query selector latency ($Q=1$); **Amort.** is per-query selector latency amortised over $Q=10$ queries on the same video.

Method	Train-Free	Query Representation	Selection Evidence	E2E Latency	Amort. Latency	Interpretability (Compositional Qs)
BOLT	✓	Global embedding	Vis.	3.0 s	0.3 s	Per-frame score
AKS	✓	Global embedding	Vis.	2.7 s	1.4 s	Per-frame score
MDP ³	✓	Global embedding	Vis.	1.8 s	0.7 s	Per-frame score
T*	✓	Flat object queries	Vis. (OVD)	13.0 s	13.0 s	Detection logs
VSLs	✓	Fixed relation triplets	Vis. (OVD)	13.3 s	13.3 s	Detection logs
NeuS-QA	✓	Temporal logic spec.	Vis.	6.7 s	6.7 s	Verification trace
VideoAgent	✗	Implicit (iterative LLM)	Vis.	44.7 s	12.3 s	None
SeViLA	✗	Implicit (per-frame VLM)	Vis.	60.0 s	60.0 s	None
VideoZoomer	✗	Implicit (iterative VLM)	Vis.	16.0 s	16.0 s	None
Frame-Voyager	✗	Learned score fn.	Vis.	1.6 s	0.2 s	None
FFS	✗	Learned policy	Vis.	0.1 s	0.1 s	None
VidF4	✗	Learned score fn.	Vis.	1.1 s	0.7 s	None
HiMu (ours)	✓	Hierarchical logic tree	Vis.+Aud.	13.3 s	9.0 s	Frame \times Expert scores

satisfaction curve; and (iv) the top- K frames are selected via PASS (Sec. 3.3). Crucially, the entire selection requires a single text-only LLM call to construct the logic tree, without incurring the latency of iterative LVLm inference calls.

3.1 Neuro-Symbolic Query Decomposition

A single text-only LLM call receives Q (with answer options, if multiple-choice) and outputs a hierarchical logic tree \mathcal{T} in structured JSON. The tree generation is a text-in, text-out forward pass. The exact system prompt and the JSON schema constraint will be provided in the supplementary. The tree has two node types:

Leaf nodes. Each leaf specifies a modality-specific expert and a text query: $\ell = (\text{expert}, \text{query})$, where $\text{expert} \in \{\text{CLIP}, \text{OVD}, \text{OCR}, \text{ASR}, \text{CLAP}\}$ and query is a natural-language atomic predicate (e.g. $\text{OVD}(\text{‘red car’})$ or $\text{ASR}(\text{‘reaction’})$). The LLM routes each predicate to the best-suited expert: actions, scenes, and abstract visual concepts \rightarrow CLIP; physical objects and people \rightarrow OVD; on-screen text \rightarrow OCR; spoken content \rightarrow ASR; environmental sounds \rightarrow CLAP. Routing rules and worked examples are provided in the system prompt; no training is required.

Internal nodes. Each internal node applies a logical or temporal operator to its children. Four operators are available:

- AND – co-occurrence: all children must be active simultaneously.
- OR – disjunction: at least one child must be active.
- SEQ – temporal sequence: children are ordered chronologically.
- RIGHAFTER – tight temporal adjacency: the effect immediately follows the cause.

MCQ tree pattern. For multiple-choice questions, the tree typically follows $\text{AND}(\text{shared_context}, \text{OR}(\text{option}_1, \dots))$, factoring elements common to all options out of the OR. Each option branch is itself decomposed

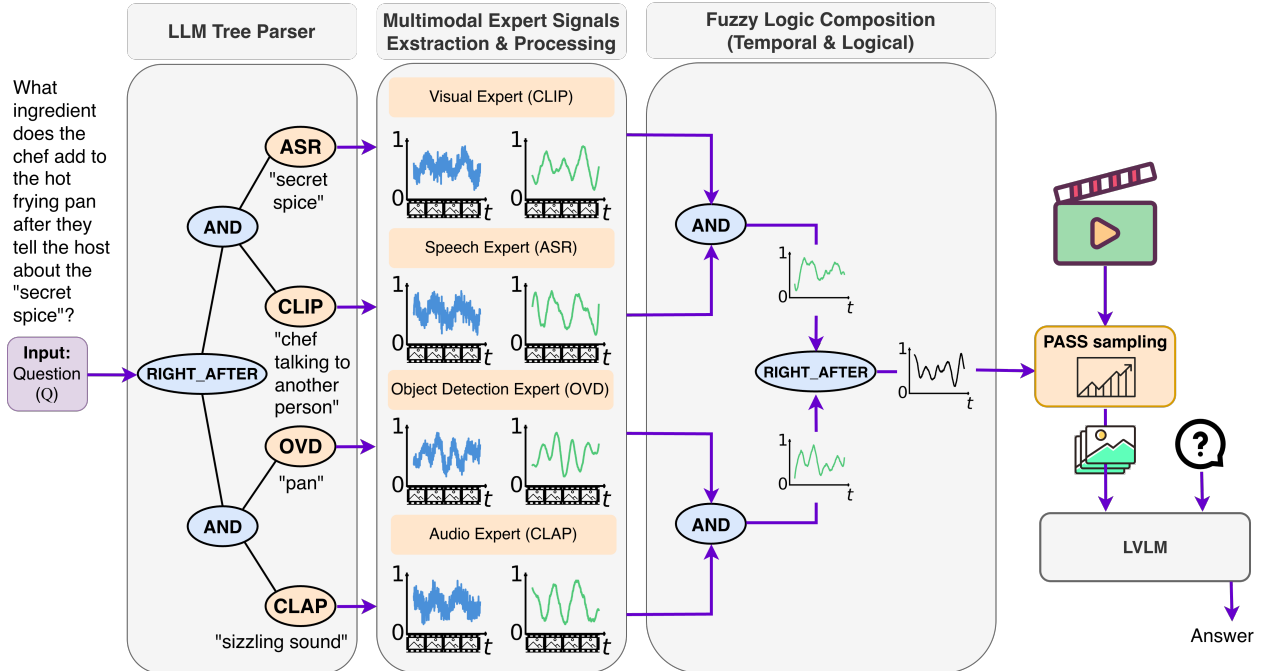


Figure 3: The HiMu pipeline. (1) An LLM parses the question into a logic tree of modality-specific experts. (2) Experts (CLIP, ASR, OVD, CLAP) extract raw signals, which are then normalized and smoothed. (3) Fuzzy logic operators compose signals into a temporal satisfaction curve. (4) Top frames are sampled for the LVLMM using PASS.

into expert-specific atomic predicates (see Fig. 4 for worked examples).

3.2 Multimodal Expert Signals Extraction and Processing

Leaf nodes are grouped by expert type for efficient batched inference. Each expert produces a per-frame raw relevance signal $u_i(t) \in \mathbb{R}$ for leaf i at every timestamp $t \in \{1, \dots, T\}$. Five experts span two modality categories; to our knowledge, no prior frame selector leverages audio experts, and we show their inclusion is critical for key-moment discovery.

Visual experts. **CLIP** [4] computes cosine similarity between frame and text-query embeddings, mapped to $[0, 1]$; frame embeddings are extracted once and shared across all CLIP leaves. **OVD** [23] runs open-vocabulary object detection, returning the maximum detection confidence for the queried class per frame; query variations (singular/plural, with/without adjectives) are generated for robust matching. **OCR** [31] performs on-screen text recognition with substring and Levenshtein-distance fuzzy matching.

Audio experts. **ASR** [32] transcribes the audio track once into timestamped word segments; queries are matched via exact substring matching (score = 1.0) or, failing that, semantic similarity via a sentence-embedding model, with segment scores mapped to frames by temporal-overlap weighting. **CLAP** [26] computes cosine similarity between frame-aligned audio chunks and the text query for non-speech sounds (environmental sounds, effects, music).

Caching and conditional execution. CLIP, ASR, CLAP, and OCR features are query-independent and cached per video; only OVD is query-conditioned and re-run per query. Unused experts are skipped entirely.

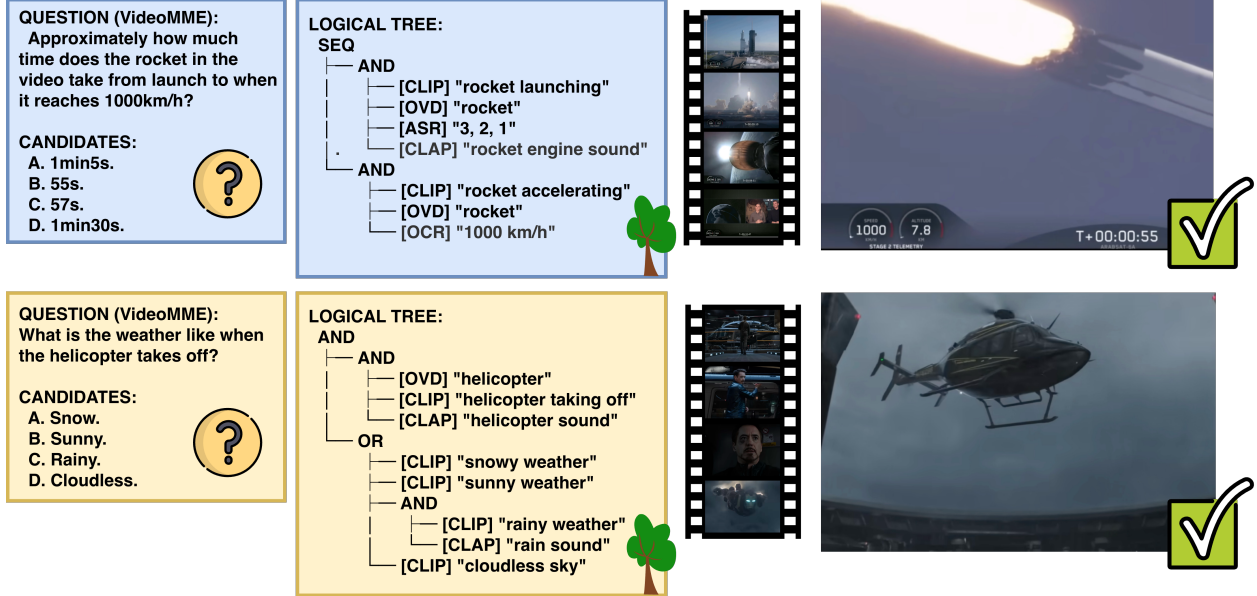


Figure 4: Logic tree examples on VideoMME questions, combining visual and audio experts.

Normalization. Raw expert scores live on incomparable scales: CLIP cosine similarities, OVD confidences, and binary ASR matches, each occupy different ranges with different noise profiles. Each signal u_i is mapped to $(0, 1)$ via:

$$\tilde{u}_i(t) = \sigma\left(\gamma \cdot \frac{u_i(t) - \text{med}(u_i)}{\text{MAD}(u_i) + \delta}\right), \quad (1)$$

where $\text{med}(\cdot)$ and $\text{MAD}(\cdot)$ denote the median and Median Absolute Deviation, $\sigma(\cdot)$ is the sigmoid, γ controls sharpness, and δ is a small stabilizer. Median/MAD provides robustness to the heavy-tailed score distributions typical of detection and retrieval models, and the sigmoid yields a smooth mapping compatible with fuzzy logic. When multiple leaves share the same expert, statistics are computed jointly from the concatenation of all their signals, preserving relative magnitude differences—otherwise, independent normalization would stretch both a high-confidence detection (e.g. 0.9 for ‘Man’) and a low-confidence one (0.2 for ‘Car’) to $[0, 1]$, falsely implying equal relevance and undermining the AND operator’s ability to down-weight weakly supported predicates.

Bandwidth-matched smoothing. After normalization, each signal is convolved with a modality-specific Gaussian kernel:

$$\hat{u}_i(t) = \sum_{t'=1}^T \tilde{u}_i(t') \mathcal{G}(t - t'; \sigma_m), \quad (2)$$

where $\mathcal{G}(\Delta; \sigma) = \frac{1}{\sqrt{2\pi}\sigma} \exp(-\Delta^2/2\sigma^2)$ and $m = \text{expert}_i$. Visual signals (CLIP, OVD, OCR) are frame-precise and receive narrow kernels; ASR and CLAP have coarser temporal resolution and receive wider kernels. This resolves cross-modal asynchrony by ensuring that peaks from different modalities overlap temporally, preventing missed conjunctions at the composition stage.

3.3 Fuzzy Logic Composition

Bottom-up tree evaluation. The logic tree \mathcal{T} is evaluated bottom-up: leaf nodes return their processed signals $\hat{u}_i(t)$; internal nodes apply continuous fuzzy-logic operators.

Logical operators (applied pairwise left-to-right for $n > 2$ children):

$$\text{AND}(A, B)(t) = A(t) \cdot B(t) \quad (\text{product t-norm}), \quad (3)$$

$$\text{OR}(A, B)(t) = A(t) + B(t) - A(t) \cdot B(t) \quad (\text{probabilistic sum}). \quad (4)$$

AND requires all children to be simultaneously active; OR is satisfied when at least one child is active.

Temporal operators.

SEQ (*temporal ordering*). Given children (u_1, \dots, u_L) in chronological order, this operator verifies that the events occur in the specified sequence and selects frames from *every* step:

$$\text{SEQ}(t) = \max_{\ell \in \{1, \dots, L\}} \left[u_\ell(t) \cdot \prod_{j < \ell} H_j(t) \cdot \prod_{j > \ell} F_j(t) \right], \quad (5)$$

where $H_j(t) = \max_{s < t} u_j(s)$ is the *has-occurred* signal (running max up to t) and $F_j(t) = \max_{s > t} u_j(s)$ is the *yet-to-occur* signal (running max after t). Intuitively, a step ℓ can only activate at time t if every earlier step has already peaked and every later step will still peak in the future. The outer max lets each step contribute its own peak, so frames from all events are selected—not just the final one.

RIGHTAFTER (*tight temporal proximity*). For cause–effect pairs that should happen close together in time, this operator scores a frame highly when the other event occurred nearby, with the score decaying exponentially with temporal distance (controlled by κ):

$$S_{\text{effect}}(t) = \text{effect}(t) \cdot \sum_{s < t} \text{cause}(s) e^{-\kappa(t-s)}, \quad (6)$$

$$S_{\text{cause}}(t) = \text{cause}(t) \cdot \sum_{s > t} \text{effect}(s) e^{-\kappa(s-t)}, \quad (7)$$

$$\text{RIGHTAFTER}(t) = \max(S_{\text{effect}}(t), S_{\text{cause}}(t)). \quad (8)$$

The two terms ensure frames are selected from both the cause and the effect side: S_{effect} scores effect frames weighted by how recently the cause fired, while S_{cause} does the reverse.

The root of \mathcal{T} produces the **satisfaction curve** $T(t) \in [0, 1]$, a per-frame composite score reflecting how well the entire logic tree is satisfied at each timestamp.

PASS: Peak-And-Spread Selection. Naïvely selecting the top- K frames of $T(t)$ often over-concentrates on a single high-scoring segment, missing other relevant events and providing little short-term motion context. We therefore introduce **PASS (Peak-And-Spread Selection)**, a peaked selection strategy with local temporal spread. We first select N_p local maxima of $T(t)$, enforcing a minimum inter-peak distance of Δ . This prevents redundant peaks while avoiding an artificial requirement to “cover” the full video timeline, which could otherwise force selecting peaks in low-satisfaction regions. Each peak is then augmented with its N_n highest-scoring neighboring frames within a local temporal window of size w centered at the peak. This captures short-term motion around each event while scaling the local context with the available budget. Finally, the remaining budget is filled greedily by selecting the highest-scoring frames from $T(t)$ among those not yet selected, allowing additional allocation to the most relevant peaks when warranted. Each selected frame v_{t^*} carries its per-leaf scores $\{\hat{u}_i(t^*)\}$, providing an interpretable trace of *which experts and predicates* drove its selection.

4 Experiments

We evaluate HiMu through the following research questions:

- **(Q1)** Does HiMu yield higher accuracy than existing similarity-based and iterative selectors when strictly constrained to the same minimal frame budget?
- **(Q2)** Can HiMu generalize as a plug-and-play module to improve diverse LVLMs, and how does its low-frame regime (16 frames) compare to multi-round methods processing heavily expanded contexts?
- **(Q3)** What is the contribution of each component of HiMu – the hierarchical composition and individual expert modalities?
- **(Q4)** How does HiMu scale with the frame budget?
- **(Q5)** What is HiMu’s computational efficiency relative to existing methods?

4.1 Setup

We evaluate HiMu on three benchmarks spanning distinct modality regimes and report accuracy, component ablations, and efficiency.

Benchmarks. We evaluated HiMu on three complementary benchmarks that cover audio, subtitles-as-speech, and visual-only settings.

- **Video-MME** [15]: 900 videos with 2,700 expert-annotated multiple-choice questions spanning 6 visual domains and 30 subfields, with durations from 11s to 1h split into Short (<2 min), Medium (4–15 min), and Long (30–60 min) subsets. Its audio tracks and explicit duration splits make it ideal for systematically evaluating HiMu’s multimodal expert pathways across temporal scales.
- **LongVideoBench_{val}** [16]: the validation split (~1.3K questions) of LongVideoBench, spanning 17 categories. Each question includes a referring query that targets specific moments, making it well-suited for evaluating moment-level retrieval and cross-modal reasoning. Videos are accompanied by subtitles (original or Whisper-transcribed), which we treat as a proxy for speech content when evaluating speech-driven selection.
- **HERBench-Lite** [17]: a 2K-question subset of HERBench-Lite spanning 12 highly compositional tasks that enforce multi-evidence integration ($m \geq 3$ non-overlapping cues), selected for its challenging reasoning demands. HERBench-Lite contains neither audio nor subtitles, providing a purely visual evaluation setting.

Implementation details. All experiments are conducted on $8 \times$ NVIDIA RTX Pro 6000 GPUs. Unless stated otherwise, we select $K=16$ frames at 1 fps sampling. HiMu is entirely training-free: the logic tree is constructed by the same LLM that serves as the downstream answering model. The default expert backbones are CLIP-dfn [33], YOLO-World v2 [23] (OVD), docTR [31] (OCR), faster-whisper large-v3-turbo [32] (ASR), and LAION CLAP [26]; features (except OVD) are extracted once per video and cached. The PASS selection strategy (Sec. 3.3) partitions the budget between peak-centered clusters that enforce temporal diversity and greedy satisfaction-based filling for the most relevant events. All hyperparameter values (γ , κ , per-modality smoothing bandwidths σ), exact PASS parameters, and a sensitivity analysis are provided in the supplementary material.

Baselines. We compare HiMu against two classes of baselines to evaluate both its direct algorithmic advantage and its standing in the broader literature. First, for a strictly controlled apples-to-

apples comparison, we fix the backbone (Qwen3-VL-8B [1]) and the frame budget ($K = 16$). Here, we compare against **Uniform Sampling** (the default strategy of most LVLMS) and three state-of-the-art selectors: two efficient similarity-based methods (**BOLT** [6] and **AKS** [7]), and an iterative detector-based approach (**T*** [22]). Because many questions in Video-MME and LongVideoBench_{val} require audio to be solvable, every method in this controlled group feeds its K selected frames together with the full video subtitles, the question, and the candidates to the same LVLMS, ensuring the selection strategy is the only variable. Second, to contextualize HiMu against computationally heavy systems, we compare against the published performance of state-of-the-art agentic and multi-round methods (**VideoZoomer** [28], **VideoChat-A1** [34], and **VSLs** [24]) paired with comparable backbones (Qwen2.5-VL 7B [35] and GPT-4o [3]). Crucially, this places HiMu at a severe numerical disadvantage: while we restrict HiMu to its standard 16 frames, these baselines consume anywhere from 32 to 512 frames per query.

4.2 Main Results

To evaluate effectiveness against frame selection baselines and generalization across LVLMS, Table 2 reports accuracy on Video-MME [15], LongVideoBench_{val} [16], and HERBench-Lite [17].

(Q1) Controlled baseline comparison. Under the strict $K=16$ budget with Qwen3-VL-8B, HiMu outperforms all competing selection strategies across every benchmark. The advantage is most pronounced on LongVideoBench (+6.70pp over T*), where resolving moment-level, cross-modal referring queries directly exposes the limits of flat similarity scoring. On Video-MME, HiMu maintains robust performance across all duration splits. On HERBench-Lite, while absolute margins are compressed by the inherent "fusion deficit" of current LVLMS [17] - an inability to integrate multiple non-overlapping evidence cues even under oracle conditions - HiMu still establishes a new state-of-the-art (43.22%), proving that precise evidence retrieval remains valuable even when downstream reasoning is bottlenecked.

(Q2) Generalization and asymmetric budget comparisons. HiMu acts as a universal plug-and-play enhancer, consistently improving over uniform sampling across six diverse LVLMS without any model-specific tuning. More importantly, HiMu achieves these gains while operating under a severe frame-budget handicap compared to existing literature. When paired with Qwen2.5-VL 7B, HiMu at just 16 frames (69.70%) comfortably outperforms both VideoZoomer operating at 128 frames (62.57%) and VideoChat-A1 at 512 frames (65.20%). We observe an even starker contrast with GPT-4o: HiMu using 16 frames reaches 78.18% on Video-MME, surpassing VSLs (67.09% with 32 frames) and VideoChat-A1 (62.99% with 384 frames). This performance difference suggests a key takeaway: retrieving a small number of precisely localized, compositionally verified frames can be more effective than expanding the LVLMS context window with hundreds of densely sampled frames.

4.3 Component Analysis and Frame Budget

(Q3) Expert and Composition Ablation. To isolate the sources of HiMu’s gains, we ablate both the composition mechanism and individual expert modalities on Video-MME (Table 3, Left).

We first replace the hierarchical logic-tree composition with a *Flat Fusion* baseline that sums leaf scores without tree structure or fuzzy-logic operators, directly isolating the contribution of compositional structure over multi-signal aggregation alone. We then conduct a leave-one-out study, removing each expert in turn.

Compositional structure is the single largest contributor to HiMu’s accuracy. Replacing the logic tree with Flat Fusion yields the steepest overall drop (−5.49pp), larger than

Table 2: Comparison of HiMu with baseline frame selection methods and its generalization across different LVLMs. We report accuracy on Video-MME (Overall, Short, Medium, Long), LongVideoBench_{val}, and HERBench-Lite. Unless stated otherwise, all methods select $K=16$ frames. Gray entries denote results reported by the respective authors under different frame budgets.

Method	Model	Video-MME				LVB _{val}	HERBench-Lite
		Short	Medium	Long	Overall		
<i>Frame Selection Baselines (Base Model: Qwen3-VL-8B)</i>							
Uniform Sampling	Qwen3-VL-8B	76.34	66.31	55.58	66.36	55.74	41.70
BOLT [6]	Qwen3-VL-8B	69.58	67.87	68.73	68.74	54.55	42.20
T* [22]	Qwen3-VL-8B	73.66	67.39	68.12	69.77	57.49	39.10
AKS [7]	Qwen3-VL-8B	70.05	65.10	68.73	67.98	57.14	40.25
HiMu (Ours)	Qwen3-VL-8B	78.55	71.00	69.90	73.22	64.19	43.22
<i>Generalization to Other LVLMs</i>							
Uniform	LLaVA-OV-1.5-8B	72.26	62.33	54.85	63.55	54.33	35.75
HiMu (Ours)	LLaVA-OV-1.5-8B	71.87	66.99	63.94	67.65	57.85	35.87
Uniform	InternVL-3.5-8B	75.41	67.39	56.55	66.63	59.23	38.30
HiMu (Ours)	InternVL-3.5-8B	76.92	70.40	66.50	71.35	64.11	38.32
Uniform	Qwen2.5-VL-7B	72.49	61.01	53.82	62.57	54.58	34.05
VideoZoomer (128 frames)	Qwen2.5-VL-7B [†]	–	–	55.8	65.2	57.7	–
VideoChat-A1 (512 frames)	Qwen2.5-VL-7B	–	–	–	69.7	55.6	–
HiMu (Ours)	Qwen2.5-VL-7B	73.08	65.10	62.86	67.09	57.51	35.17
Uniform	Gemma-3-12B	73.31	60.29	55.83	62.99	47.59	31.20
HiMu (Ours)	Gemma-3-12B	71.56	65.70	67.48	68.28	53.92	31.47
<i>Proprietary LVLMs (evaluated on a stratified random 25% subset of each benchmark)</i>							
Uniform	Gemini-2.5-Flash	78.43	67.11	61.22	68.95	56.33	37.27
HiMu (Ours)	Gemini-2.5-Flash	78.92	75.00	74.49	76.11	70.13	37.68
Uniform	GPT-4o	76.96	73.03	71.43	73.81	55.58	37.47
VLS (32 frames)	GPT-4o	71.9	61.9	55.2	63.0	63.4	–
VideoChat-A1 (384 frames)	–	–	–	–	77.2	66.7	–
HiMu (Ours)	GPT-4o	80.88	77.19	76.53	78.18	65.10	40.68

[†] Finetuned model.

removing any individual expert—demonstrating that *how* signals are composed matters more than *which* signals are present. Among individual experts, removing ASR causes the largest overall degradation (−1.99pp), followed by CLIP (−1.43pp)—a result that directly validates our claim that audio is a first-class selection modality, not merely a downstream supplement. Notably, ASR and CLIP together account for the dominant share of per-expert gains, with ASR’s effect concentrated on Short videos where spoken cues are densely informative. CLAP, OVD, and OCR contribute smaller but consistent improvements (−1.00, −0.76, and −1.04pp respectively), confirming that each modality covers a distinct slice of query-relevant evidence.

In the supplementary material, we provide a sensitivity analysis that independently isolates three factors: hyperparameter values, the choice of expert backbone (swapping each expert’s underlying model separately), and the backbone LLM used for tree parsing — evaluating the effect of each on downstream VideoQA accuracy.

(Q4) Frame Budget Analysis. We vary $K \in \{8, 16, 32, 64\}$ for both HiMu and uniform sampling (Table 3, Right). HiMu consistently outperforms uniform sampling at every budget level, with the gap peaking at $K=8$ – precisely where the cost of selecting uninformative frames is highest. **Most strikingly, HiMu at $K=16$ exceeds uniform sampling at $K=64$,** a $4\times$ reduction in the required frame budget for comparable accuracy. This result directly quantifies the waste in uniform sampling: the majority of its frames fall in query-irrelevant segments that HiMu’s compositional selection avoids entirely. The gap remains substantial even at $K=64$, confirming that query-aware

Table 3: Ablation studies on Video-MME using Qwen3-VL-8B. **Left:** Expert ablation ($K=16$). “Flat Fusion” replaces the logic tree with a flat summation of all leaf scores; each “w/o” row removes one expert. **Right:** Effect of frame budget K . HiMu at $K=16$ rivals Uniform at $K=64$.

Configuration	Video-MME			
	Short	Med.	Long	Overall
HiMu	78.55	71.00	69.90	73.22
Flat Fusion	68.65	66.06	68.45	67.73
w/o ASR	76.34	69.07	68.08	71.23
w/o CLAP	77.97	69.43	69.05	72.22
w/o CLIP	76.46	69.55	69.17	71.79
w/o OCR	77.39	69.92	69.05	72.18
w/o OVD	77.39	70.64	69.17	72.46

# Frames	Method	Video-MME			
		Short	Med.	Long	Overall
8	Uniform	73.54	63.42	54.67	64.00
	HiMu	73.54	68.71	68.81	70.39
16	Uniform	76.34	66.31	55.58	66.36
	HiMu	78.55	71.00	69.90	73.22
32	Uniform	81.35	69.19	58.67	69.89
	HiMu	80.77	73.29	70.02	74.77
64	Uniform	82.87	71.12	60.61	71.68
	HiMu	82.40	73.53	71.12	75.77

selection continues to add value well beyond tight-budget regimes.

4.4 Efficiency Analysis

(Q5) While HiMu requires significantly fewer frames to reach high accuracy, this advantage is only meaningful if the selection process itself is computationally lightweight. Figure 2 maps the accuracy-compute Pareto front on Video-MME, revealing a sharp trade-off in prior work. Similarity-based selectors [6, 7] operate with minimal overhead but typically plateau at lower accuracies. Conversely, agentic and per-frame methods [10, 11] achieve strong performance but incur substantial latency (often 3-100× higher) due to their reliance on iterative LVLM calls.

HiMu advances this Pareto front by decoupling compositional reasoning from LVLM inference. While evaluating an initial query incurs a modest cost to extract expert signals, this processing is performed only once per video. Crucially, because these features are cached, the selection latency for any subsequent query drops to a mere fraction of the initial overhead. This substantial reduction in amortized cost makes HiMu highly practical for real-world, multi-query applications. We provide a comprehensive, quantitative breakdown of these end-to-end execution times in the supplementary material. Ultimately, HiMu demonstrates that effective frame selection does not necessitate costly agentic loops.

5 Discussion

HiMu demonstrates that compositional frame selection need not require iterative LVLM inference. By decomposing queries into hierarchical logic trees evaluated by modality-specific experts - including, for the first time, audio - it identifies the most informative frames in a single shot, outperforming similarity-based selectors and matching or exceeding agent-based systems at a fraction of their cost across all three benchmarks.

The ablations pinpoint *why* existing selectors fall short. Replacing the logic tree with a flat signal sum produces the largest accuracy drop, confirming that compositional structure is the missing capability. The frame-budget analysis reinforces this: HiMu at $K=16$ exceeds uniform sampling at $K=64$, implying that most uniformly sampled frames land in query-irrelevant segments. The bottleneck in frame selection, then, lies more in how queries are represented, rather than in how many model calls are made.

Limitations. Despite its unique capabilities, HiMu has several limitations. First, it introduces higher latency than similarity-based methods due to the expert extraction stage, although amortization over multiple queries substantially mitigates this cost. Second, the pipeline heavily relies on the LLM parser producing faithful decompositions; malformed or overly shallow trees can misroute predicates and degrade selection quality. Finally, the ASR expert is bounded by the language coverage of the underlying speech model, limiting effectiveness on multilingual or low-resource audio tracks.

References

- [1] Shuai Bai, Keqin Chen, Xuejing Liu, Jialin Wang, Wenbin Ge, Sibao Song, et al. Qwen3-VL technical report. *arXiv preprint arXiv:2511.21631*, 2025.
- [2] Zhe Chen, Jiannan Wu, Wenhai Wang, Weijie Su, Guo Chen, Sen Xing, Muyan Zhong, Qinglong Zhang, Xizhou Zhu, Lewei Lu, Bin Li, Ping Luo, Tong Lu, Yu Qiao, and Jifeng Dai. Internvl: Scaling up vision foundation models and aligning for generic visual-linguistic tasks. In *Proceedings of the IEEE/CVF Conference on Computer Vision and Pattern Recognition (CVPR)*, pages 24185–24198, June 2024.
- [3] OpenAI, Aaron Hurst, Adam Lerer, et al. GPT-4o system card. *arXiv preprint arXiv:2410.21276*, 2024.
- [4] Alec Radford, Jong Wook Kim, Chris Hallacy, Aditya Ramesh, Gabriel Goh, Sandhini Agarwal, Girish Sastry, Amanda Askell, Pamela Mishkin, Jack Clark, et al. Learning transferable visual models from natural language supervision. In *International Conference on Machine Learning*, pages 8748–8763, 2021.
- [5] Xiaohua Zhai, Basil Mustafa, Alexander Kolesnikov, and Lucas Beyer. Sigmoid loss for language image pre-training. In *Proceedings of the IEEE/CVF International Conference on Computer Vision (ICCV)*, pages 11975–11986, October 2023.
- [6] Shuming Liu, Chen Zhao, Tianqi Xu, and Bernard Ghanem. Bolt: Boost large vision-language model without training for long-form video understanding. In *Proceedings of the IEEE/CVF Conference on Computer Vision and Pattern Recognition (CVPR)*, pages 3318–3327, June 2025.
- [7] Xi Tang, Jihao Qiu, Lingxi Xie, Yunjie Tian, Jianbin Jiao, and Qixiang Ye. Adaptive keyframe sampling for long video understanding. In *Proceedings of the IEEE/CVF Conference on Computer Vision and Pattern Recognition (CVPR)*, pages 29118–29128, June 2025.
- [8] Hui Sun, Shiyin Lu, Huanyu Wang, Qing-Guo Chen, Zhao Xu, Weihua Luo, Kaifu Zhang, and Ming Li. Mdp3: A training-free approach for list-wise frame selection in video-llms. In *Proceedings of the IEEE/CVF International Conference on Computer Vision (ICCV)*, pages 24090–24101, October 2025.
- [9] Yue Fan, Xiaojian Ma, Rujie Wu, Yuntao Du, Jiaqi Li, Zhi Gao, and Qing Li. Videoagent: A memory-augmented multimodal agent for video understanding. In *Computer Vision – ECCV 2024: 18th European Conference, Milan, Italy, September 29 – October 4, 2024, Proceedings, Part XXII*, pages 75–92, Berlin, Heidelberg, 2024. Springer-Verlag.

- [10] Xuan Wang, Yiming Zhang, Omer Zohar, and Sivan Yeung-Levy. Videoagent: Long-form video understanding with large language model as agent. In *European Conference on Computer Vision (ECCV)*, pages 58–76, 2024.
- [11] Boyu Chen, Zhengrong Yue, Siran Chen, Zikang Wang, Yang Liu, Peng Li, and Yali Wang. LVAgent: Long video understanding by multi-round dynamical collaboration of MLLM agents. In *Proceedings of the IEEE/CVF International Conference on Computer Vision (ICCV)*, pages 20237–20246, October 2025.
- [12] Runtao Liu, Ziyi Liu, Jiaqi Tang, Yue Ma, Renjie Pi, Jipeng Zhang, and Qifeng Chen. Longvideoagent: Multi-agent reasoning with long videos. *arXiv preprint arXiv:2512.20618*, 2025.
- [13] Shoubin Yu, Jaemin Cho, Prateek Yadav, and Mohit Bansal. SeViLA: Self-chained video localization and answering via llm. In *Advances in Neural Information Processing Systems*, 2023.
- [14] Yuanhao Zou, Shengji Jin, Andong Deng, Youpeng Zhao, Jun Wang, and Chen Chen. A.i.r.: Enabling adaptive, iterative, and reasoning-based frame selection for video question answering. In *The Fourteenth International Conference on Learning Representations*, 2026.
- [15] Chaoyou Fu, Yuhan Dai, Yongdong Luo, Lei Li, Shuhuai Ren, Renrui Zhang, Zihan Wang, Chenyu Zhou, Yunhang Shen, Mengdan Zhang, et al. Video-MME: The first-ever comprehensive evaluation benchmark of multi-modal LLMs in video analysis. In *Advances in Neural Information Processing Systems*, 2024.
- [16] Haoning Wu, Dongxu Li, Bei Chen, and Junnan Li. LongVideoBench: A benchmark for long-context interleaved video-language understanding. In *Advances in Neural Information Processing Systems*, volume 37, pages 28828–28857, 2024.
- [17] Dan Ben-Ami, Gabriele Serussi, Kobi Cohen, and Chaim Baskin. HERBench: A benchmark for multi-evidence integration in video question answering. In *Proceedings of the IEEE/CVF Conference on Computer Vision and Pattern Recognition (CVPR)*, 2026.
- [18] Sicheng Yu, Chengkai Jin, Huanyu Wang, Zhenghao Chen, Sheng Jin, Zhongrong Zuo, Xiaolei Xu, Zhenbang Sun, Bingni Zhang, Jiawei Wu, Hao Zhang, and Qianru Sun. Frame-voyager: Learning to query frames for video large language models. In *The Thirteenth International Conference on Learning Representations*, 2025.
- [19] Shyamal Buch, Arsha Nagrani, Anurag Arnab, and Cordelia Schmid. Flexible frame selection for efficient video reasoning. In *Proceedings of the IEEE/CVF Conference on Computer Vision and Pattern Recognition (CVPR)*, pages 29071–29082, June 2025.
- [20] Kai Hu, Feng Gao, Xiaohan Nie, Peng Zhou, Son Tran, Tal Neiman, Lingyun Wang, Mubarak Shah, Raffay Hamid, Bing Yin, and Trishul Chilimbi. M-LLM based video frame selection for efficient video understanding. In *Proceedings of the IEEE/CVF Conference on Computer Vision and Pattern Recognition (CVPR)*, pages 13702–13712, 2025.
- [21] Jianxin Liang, Xiaojun Meng, Yueqian Wang, Chang Liu, Qun Liu, and Dongyan Zhao. End-to-end videoqa with frame scoring mechanisms and adaptive sampling. In *Natural Language Processing and Chinese Computing (NLPCC 2025)*, volume 16103 of *Lecture Notes in Computer Science*, pages 141–154. Springer, Singapore, 2026.

- [22] Jinhui Ye, Zihan Wang, Haosen Sun, Keshigeyan Chandrasegaran, Zane Durante, Cristobal Eyzaguirre, Yonatan Bisk, Juan Carlos Niebles, Ehsan Adeli, Li Fei-Fei, Jiajun Wu, and Manling Li. Re-thinking temporal search for long-form video understanding. In *Proceedings of the IEEE/CVF Conference on Computer Vision and Pattern Recognition (CVPR)*, pages 8579–8591, June 2025.
- [23] Tianheng Cheng, Lin Song, Yixiao Ge, Wenyu Liu, Xinggang Wang, and Ying Shan. YOLO-World: Real-time open-vocabulary object detection. In *Proceedings of the IEEE/CVF Conference on Computer Vision and Pattern Recognition*, pages 16901–16911, 2024.
- [24] Weiyu Guo, Ziyang Chen, Shaoguang Wang, Jianxiang He, Yijie Xu, Jinhui Ye, Ying Sun, and Hui Xiong. Logic-in-frames: Dynamic keyframe search via visual semantic-logical verification for long video understanding. In *The Thirty-ninth Annual Conference on Neural Information Processing Systems*, 2025.
- [25] Sahil Shah, S P Sharan, Harsh Goel, Minkyu Choi, Mustafa Munir, Manvik Pasula, Radu Marculescu, and Sandeep Chinchali. Neus-qa: Grounding long-form video understanding in temporal logic and neuro-symbolic reasoning. *arXiv preprint arXiv:2509.18041*, 2025.
- [26] Yusong Wu, Ke Chen, Tianyu Zhang, Yuchen Hui, Taylor Berg-Kirkpatrick, and Shlomo Dubnov. Large-scale contrastive language-audio pretraining with feature fusion and keyword-to-caption augmentation. In *IEEE International Conference on Acoustics, Speech and Signal Processing (ICASSP)*, pages 1–5, 2023.
- [27] Ziyang Wang, Shoubin Yu, Elias Stengel-Eskin, Jaehong Yoon, Feng Cheng, Gedas Bertasius, and Mohit Bansal. VideoTree: Adaptive tree-based video representation for LLM reasoning on long videos. In *Proceedings of the IEEE/CVF Conference on Computer Vision and Pattern Recognition (CVPR)*, pages 3272–3283, June 2025.
- [28] Yang Ding, Xin Lai, Yizhen Zhang, Wei Li, Ruihang Chu, and Yujiu Yang. Videozoomer: Reinforcement-learned temporal focusing for long video reasoning. In *The Fourteenth International Conference on Learning Representations*, 2026.
- [29] Xiaoqian Shen, Yunyang Xiong, Changsheng Zhao, Lemeng Wu, Jun Chen, Chenchen Zhu, Zechun Liu, Fanyi Xiao, Balakrishnan Varadarajan, Florian Bordes, Zhuang Liu, Hu Xu, Hyunwoo J. Kim, Bilge Soran, Raghuraman Krishnamoorthi, Mohamed Elhoseiny, and Vikas Chandra. LongVU: Spatiotemporal adaptive compression for long video-language understanding. In *Forty-second International Conference on Machine Learning*, 2025.
- [30] Liang Chen, Haozhe Zhao, Tianyu Liu, Shuai Bai, Junyang Lin, Chang Zhou, and Baobao Chang. An image is worth 1/2 tokens after layer 2: Plug-and-play inference acceleration for large vision-language models. In *Computer Vision – ECCV 2024: 18th European Conference, Milan, Italy, September 29–October 4, 2024, Proceedings, Part LXXXI*, pages 19–35, Berlin, Heidelberg, 2024. Springer-Verlag.
- [31] Mindee. docTR: Document text recognition, 2021. Open-source OCR library.
- [32] Alec Radford, Jong Wook Kim, Tao Xu, Greg Brockman, Christine Mcleavey, and Ilya Sutskever. Robust speech recognition via large-scale weak supervision. In *Proceedings of the 40th International Conference on Machine Learning*, pages 28492–28518, 2023.

- [33] An Fang, Andrew M Jose, Anmol Jain, Ludwig Schmidt, Alexander Toshev, and Vaishaal Shankar. Data filtering networks. In *International Conference on Learning Representations*, 2024.
- [34] Zikang Wang, Boyu Chen, Zhengrong Yue, Yi Wang, Yu Qiao, Limin Wang, and Yali Wang. VideoChat-A1: Thinking with long videos by chain-of-shot reasoning. *arXiv preprint arXiv:2506.06097*, 2025.
- [35] Shuai Bai, Keqin Chen, Xuejing Liu, Jialin Wang, Wenbin Ge, Siboz Song, Kai Dang, Peng Wang, Shijie Wang, Jun Tang, Humen Zhong, Yuanzhi Zhu, Mingkun Yang, Zhaohai Li, Jianqiang Wan, Pengfei Wang, Wei Ding, Zheren Fu, Yiheng Xu, Jiabo Ye, Xi Zhang, Tianbao Xie, Zesen Cheng, Hang Zhang, Zhibo Yang, Haiyang Xu, and Junyang Lin. Qwen2.5-VL technical report. *arXiv preprint arXiv:2502.13923*, 2025.
- [36] Shilong Liu, Zhaoyang Zeng, Tianhe Ren, Feng Li, Hao Zhang, Jie Yang, Qing Jiang, Chunyuan Li, Jianwei Yang, Hang Su, Jun Zhu, and Lei Zhang. Grounding DINO: Marrying DINO with grounded pre-training for open-set object detection. In *European Conference on Computer Vision (ECCV)*, 2024.
- [37] JaidedAI. EasyOCR: Ready-to-use OCR with 80+ supported languages, 2020.
- [38] Xiang An, Yin Xie, Kaicheng Yang, Wenkang Zhang, Xiuwei Zhao, Zheng Cheng, Yirui Wang, Songcen Xu, Changrui Chen, Chunsheng Wu, Huaqie Tan, Chunyuan Li, Jing Yang, Jie Yu, Xiyao Wang, Bin Qin, Yumeng Wang, Zizhen Yan, Ziyong Feng, Ziwei Liu, Bo Li, and Jiankang Deng. LLaVA-OneVision-1.5: Fully open framework for democratized multimodal training. *arXiv preprint arXiv:2509.23661*, 2025.
- [39] Gemini Team, Google. Gemini 2.5: Pushing the frontier with advanced reasoning, multimodality, long context, and next generation agentic capabilities. *arXiv preprint arXiv:2507.06261*, 2025.
- [40] Weiyun Wang, Zhangwei Gao, Lixin Gu, Hengjun Pu, Long Cui, Xingguang Wei, Zhaoyang Liu, Linglin Jing, Shenglong Ye, Jie Shao, et al. InternVL3.5: Advancing open-source multimodal models in versatility, reasoning, and efficiency. *arXiv preprint arXiv:2508.18265*, 2025.

HiMu: Hierarchical Multimodal Frame Selection for Long Video Question Answering — Supplementary Material

Contents

A Neuro-Symbolic Query Decomposition Details	18
B Implementation Details	20
C PASS Algorithm	20
D Sensitivity Analysis	23
E Selector Latency Breakdown	26
F Interpretability of Frame Selection	27

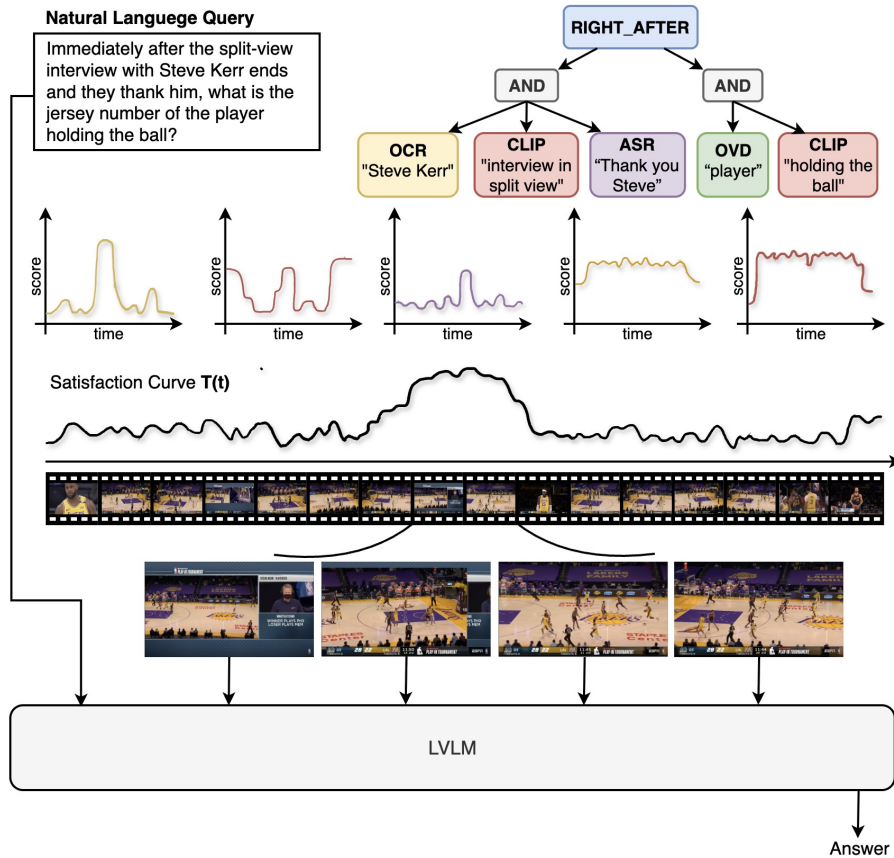


Figure 5: **HiMu pipeline overview.** Given a natural-language query, an LLM decomposes it into a hierarchical logic tree whose leaves are routed to modality-specific experts (OCR, CLIP, ASR, OVD, CLAP). Each expert produces a per-frame relevance signal over time; these signals are composed bottom-up via fuzzy-logic operators into a satisfaction curve $T(t)$. The top-scoring frames are selected and passed to the LVL for answering.

A Neuro-Symbolic Query Decomposition Details

A.1 System Prompt for Tree Generation

The system prompt guides the LLM to decompose each question into a hierarchical logic tree. Because different benchmarks provide different audio modalities, the prompt is adapted per benchmark by enabling or disabling expert descriptions and their associated rules. We first present the *common* prompt shared across all benchmarks (Listing 1), then summarize the per-benchmark adaptations in Table 4.

Listing 1: Common system prompt for logic tree generation (shared across all benchmarks). Sections marked [IF_ASR] and [IF_CLAP] are included only when the corresponding expert is enabled (see Table 4).

```
You are a Neuro-Symbolic Logic Parser for a Multimodal
Video Understanding system. Convert Video QA questions into
structured logical trees that leverage ALL relevant modalities.

### THE EXPERTS

**Visual Experts:**
1. **OVD** - Open-Vocabulary Object Detection (YOLO-World)
  - For: Physical objects, people, and visual attributes
  - Examples: "person", "car", "dog", "red car", "man in suit"
  - Supports attribute+noun phrases. Never include numbers,
    counts, or proper names.
  - OVD CANNOT detect: countries, teams, names, states,
    emotions, actions, text, numbers

2. **OCR** - On-Screen Text Recognition
  - For: Text visible on screen - signs, labels, jersey
    numbers, names, scoreboards
  - Examples: "Exit", "10", "Warning", "Korea"

3. **CLIP** - Semantic Visual Understanding
  - For: Actions, scenes, visual states, atmosphere, abstract
    visual concepts
  - CLIP is VISUAL ONLY - queries must describe something you
    can SEE in a video frame
  - Good: "person speaking", "diagram on screen", "cooking"
  - Bad: "quantum entanglement", "innovation"
    (invisible concepts)

[IF_ASR]
4. **ASR** - Speech Recognition
  - For: Spoken words, dialogue, narration, verbal references
  - Use SHORT keywords (1-3 words), never full sentences
  - CRITICAL: People TALK about what is shown. Add an ASR
    leaf with related spoken keywords alongside visual leaves.
[/IF_ASR]

[IF_CLAP]
5. **CLAP** - Environmental Audio Events
  - For: Non-speech sounds, music, sound effects, ambient audio
  - Examples: "doorbell ringing", "applause", "glass breaking"
[/IF_CLAP]

### THE OPERATORS

- **AND**: All children must co-occur (same frame).
- **OR**: At least one child satisfied.
- **SEQ**: Temporal sequence (earliest first, latest last).
  ONLY when order is EXPLICITLY STATED.
  IMPORTANT: If the question ASKS about order/sequence,
```

Table 4: Per-benchmark prompt adaptations for HiMu’s logic-tree parser. The common prompt (Listing 1) is shared across all benchmarks; only the dimensions shown below differ per benchmark.

	Video-MME	LongVideoBench	HERBench
Active experts	OVD, OCR, CLIP, ASR, CLAP	OVD, OCR, CLIP, ASR	OVD, OCR, CLIP
[IF_ASR] included	✓	✓	✗
[IF_CLAP] included	✓	✗	✗
Rules 2, 12–14	✓	✓	✗
Prompt examples	4 (audio, OCR+ASR, multimodal, temporal)	3 (speech, scientific, temporal)	3 (MCQ, ordering, OCR+visual)

```

do NOT use SEQ. Instead: build one AND per shot,
wrap in a flat OR. Each shot appears exactly once.
- **RIGHT_AFTER**: Immediate temporal succession.
  Exactly 2 children [cause, effect].

### KEY RULES

1. MULTIMODAL: Each MCQ option should combine more than one expert type,
  [IF_ASR: visual AND audio evidence when possible. Never make a tree
  with only one expert type.] [ELSE: Use multiple visual
  experts when possible.]
[IF_ASR]
2. ASR OVERLAP: Add ASR leaves with short keywords alongside
  visual leaves - narrators often describe what is shown.
[/IF_ASR]
3. MCQ STRUCTURE: AND(shared_context, OR(opt_1, opt_2, ...))
  - factor shared elements OUT of the OR.
4. DECOMPOSE RICH DESCRIPTIONS: Create separate leaves for
  each element: OVD for objects/people, CLIP for
  settings/states.
5. SEQ ONLY FOR KNOWN ORDER.
6. NAMES -> OCR [IF_ASR: + ASR (spoken)].
7. VISUAL STATES -> CLIP, not ASR alone.
8. META-OPTIONS: "Same", "All of the above", etc. ->
  ALWAYS skip in the OR.
9. ACTIONS IN OPTIONS: AND(OVD:object, CLIP:action).
10. TEMPORAL CAUSE: cause child = action (CLIP), not person.
11. OVERLAPPING EXPERTS encouraged.
[IF_ASR]
12. VISUAL GROUNDING: Never build ASR-only options.
13. OVERLAPPING PREDICATES: Mix experts with overlapping
  terms for robust detection.
14. SUBTITLES -> ASR + OCR.
[/IF_ASR]

### OUTPUT FORMAT
Return a single JSON object:
{"op": "AND"|"OR"|"SEQ"|"RIGHT_AFTER"|"LEAF",
 "children": [...],
 "expert": <available experts>, "query": "string"}

```

The prompt also includes 3–4 worked examples tailored to each benchmark’s modality regime (e.g., CLAP-based examples for Video-MME, speech-triggered examples for LongVideoBench, visual-only examples for HERBench). The complete per-benchmark prompts including all examples are

provided in our code repository.

A.2 JSON Schema Constraint

The LLM output is constrained to valid JSON matching the following schema. Leaf nodes carry `expert` and `query` fields; internal nodes carry an `op` and a `children` array.

Listing 2: JSON schema for logic tree output.

```
{
  "op": "AND" | "OR" | "SEQ" | "RIGHT_AFTER" | "LEAF",
  "children": [<recursive tree nodes>], // non-LEAF only
  "expert": "CLIP"|"OVD"|"OCR"|"ASR"|"CLAP", // LEAF only
  "query": "<atomic predicate string>" // LEAF only
}
```

The available values for `expert` are restricted per benchmark to match the active expert set (Table 4).

A.3 Expert Routing Rules

The system prompt encodes the following routing logic, which the LLM applies when assigning predicates to experts:

- **Physical objects and people** → OVD (e.g., “red car”, “man in suit”).
- **Actions, scenes, visual states** → CLIP (e.g., “person running”, “sunset”).
- **On-screen text** → OCR (e.g., “Exit”, “Warning”, jersey numbers).
- **Spoken content and dialogue** → ASR (e.g., “reaction”, “careful”).
- **Environmental sounds** → CLAP (e.g., “applause”, “glass breaking”).
- **Proper names** → OCR + ASR (text on screen and spoken references).
- **Actions with objects** → AND(OVD:object, CLIP:action) for robust detection.

Worked example. For the question “*After the doorbell rings, who opens the door?*” with options [“A man”, “A woman”]:

- “doorbell rings” → CLAP (environmental sound event).
- “opens the door” → CLIP (action/visual state).
- “A man” / “A woman” → OVD (physical person detection).
- Temporal cue “after” → SEQ operator wrapping the cause (doorbell) before the effect (door opening + person).

B Implementation Details

Table 5 lists all hyperparameter values used throughout the paper. Parameters are grouped by the pipeline stage they belong to, with references to the corresponding equations and sections in the main paper.

C PASS Algorithm

Algorithm 1 provides the pseudocode for PASS (Peak-And-Spread Selection). Phase 1 identifies N_p prominent peaks in the satisfaction curve while enforcing a minimum temporal separation of Δ frames, preventing redundant selection from a single high-scoring segment without artificially requiring coverage of the full timeline. Phase 2 augments each peak with its N_n highest-scoring

Table 5: Complete hyperparameter settings for HiMu.

Parameter	Symbol	Value	Description
<i>Normalization (Eq. 1, Sec. 3.2 in the main paper)</i>			
Sigmoid sharpness	γ	3.0	Steepness of the sigmoid in median/MAD normalization; higher values sharpen contrast between high- and low-scoring frames
MAD stabilizer	δ	10^{-6}	Prevents division by zero when all expert scores are identical (MAD = 0)
<i>Temporal operators (Eqs. 6–8, Sec. 3.3 in the main paper)</i>			
RightAfter decay	κ	2.0	Exponential decay for the RIGHTAFTER operator; larger values restrict cause–effect pairing to closer frames
<i>Bandwidth-matched smoothing (Eq. 2, Sec. 3.2 in the main paper)</i>			
CLIP smoothing	σ_{clip}	0.5	Narrow kernel for frame-precise visual similarity scores
OVD smoothing	σ_{ovd}	0.5	Narrow kernel for frame-precise object detection confidences
OCR smoothing	σ_{ocr}	0.5	Narrow kernel for frame-precise on-screen text detections
ASR smoothing	σ_{asr}	1.5	Wider kernel to bridge coarser temporal resolution of speech transcripts
CLAP smoothing	σ_{clap}	2.0	Widest kernel for coarse temporal granularity of audio events
<i>PASS selection (Sec. 3.3 in the main paper)</i>			
Number of peaks	N_p	$\lfloor \sqrt{K} \rfloor$	Scales sub-linearly with K to encourage coverage of multiple relevant events
Neighbors per peak	N_n	$\lfloor \sqrt{K}/2 \rfloor$	Neighbors per peak capturing fine-grained details and short-term temporal changes
Local window size	w	$\lfloor \sqrt{K} \rfloor$	Neighbor search window width ($\lfloor w/2 \rfloor$ per side); equals Δ to prevent overlap between peak neighborhoods
Min inter-peak distance	Δ	$\lfloor \sqrt{K} \rfloor$	Minimum frame separation between peaks; equals N_p to ensure non-overlapping neighborhoods and diverse coverage

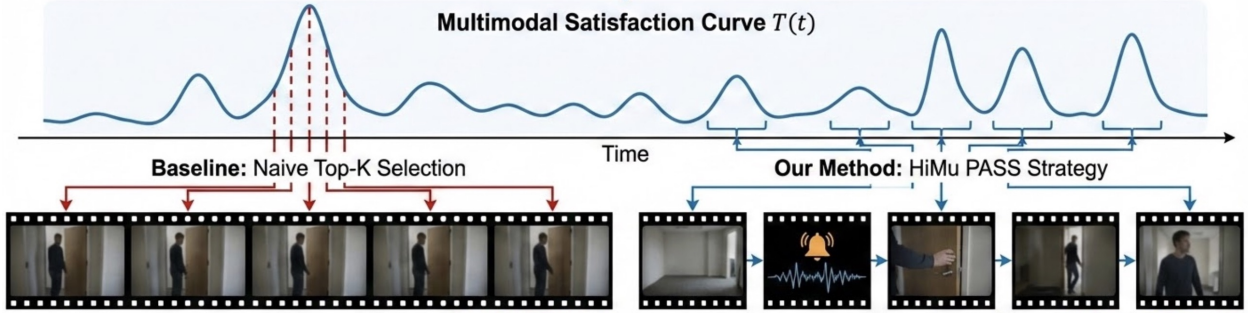


Figure 6: **PASS vs. naive top- K selection.** Given the multimodal satisfaction curve $T(t)$, naive top- K (left, red) concentrates all selected frames around the single highest peak, missing other relevant events. PASS (right, blue) detects multiple peaks, spreads neighbors around each, and fills the remaining budget greedily, yielding diverse temporal coverage.

neighbors within a local window of w frames, capturing short-term motion context. Phase 3 fills the remaining budget greedily from the highest-scoring unselected frames.

PASS vs. vanilla top- K . As illustrated in Fig. 6, on a random 50% subset of Video-MME (Qwen3-VL-8B, $K=16$), PASS achieves 73.31% compared to 72.59% for vanilla top- K selection (+0.72pp). Vanilla top- K tends to concentrate all selected frames within a single high-scoring segment, missing relevant events elsewhere in the video. PASS mitigates this by explicitly detecting multiple peaks and spreading neighbors around each, ensuring coverage of distinct temporal events while preserving fine-grained context around each key moment.

Algorithm 1 PASS: Peak-And-Spread Selection

Require: Satisfaction curve $T(t)$ for $t \in \{1, \dots, T\}$, frame budget K , number of peaks N_p , neighbors per peak N_n , window size w , min inter-peak distance Δ

Ensure: Selected frame indices \mathcal{S} with $|\mathcal{S}| = K$

```
1:  $\mathcal{S} \leftarrow \emptyset$ 
2:
3: // Phase 1: Peak detection
4:  $\mathcal{P} \leftarrow \emptyset$  // set of selected peak indices
5:  $\mathcal{C} \leftarrow \{t : T(t) > T(t-1) \text{ and } T(t) > T(t+1)\}$  // find all local maxima in the satisfaction curve
6: Sort  $\mathcal{C}$  by  $T(t)$  in descending order // process highest-scoring peaks first
7: for  $t \in \mathcal{C}$  do
8:   if  $|t - t'| \geq \Delta$  for all  $t' \in \mathcal{P}$  then
9:      $\mathcal{P} \leftarrow \mathcal{P} \cup \{t\}$  // enforce min separation: skip peaks too close to existing ones
10:  end if
11:  if  $|\mathcal{P}| = N_p$  then
12:    break // enough diverse peaks collected
13:  end if
14: end for
15:  $\mathcal{S} \leftarrow \mathcal{S} \cup \mathcal{P}$ 
16:
17: // Phase 2: Neighbor spread // add nearby frames around each peak to capture local temporal context
18: for each peak  $p \in \mathcal{P}$  do
19:    $\mathcal{W}_p \leftarrow \{t : |t - p| \leq \lfloor w/2 \rfloor, t \notin \mathcal{S}\}$  // candidate neighbors within window  $w$  around peak  $p$ 
20:   Sort  $\mathcal{W}_p$  by  $T(t)$  in descending order
21:    $\mathcal{S} \leftarrow \mathcal{S} \cup \mathcal{W}_p[1 : N_n]$  // keep top- $N_n$ : best context frames around this peak
22: end for
23:
24: // Phase 3: Greedy fill // use remaining budget on highest-scoring uncovered frames
25:  $\mathcal{R} \leftarrow \{1, \dots, T\} \setminus \mathcal{S}$  // frames not yet selected
26: Sort  $\mathcal{R}$  by  $T(t)$  in descending order
27:  $\mathcal{S} \leftarrow \mathcal{S} \cup \mathcal{R}[1 : (K - |\mathcal{S}|)]$  // fill to budget  $K$ 
28: return  $\mathcal{S}$ 
```

D Sensitivity Analysis

All sensitivity experiments use Qwen3-VL-8B as the downstream LVLM with $K=16$ frames on a random 50% subset of Video-MME (1,244 questions). The subset is stratified by video duration and question category and held fixed across all ablation conditions in this section. Each experiment changes exactly one component from the default configuration, isolating the contribution of each design choice.

D.1 Hyperparameter Sensitivity

We systematically vary the smoothing bandwidths, temporal decay factor, and sigmoid sharpness one at a time (Table 6). All perturbations remain within at most 1.04 pp of the baseline, confirming that HiMu is not tightly coupled to any single hyperparameter setting. This stability stems from

Table 6: Hyperparameter sensitivity on a random 50% subset of Video-MME (Qwen3-VL-8B, $K=16$). Each row changes one hyperparameter from the default. Δ is the difference from the baseline.

Configuration	Accuracy	Δ
HiMu (default)	73.31	—
<i>Smoothing bandwidths</i>		
All smoothing disabled	73.23	-0.08
Visual σ (CLIP/OVD/OCR, default: 0.5) \rightarrow 0	73.23	-0.08
Visual σ (CLIP/OVD/OCR, default: 0.5) \rightarrow 2	72.27	-1.04
Speech σ (ASR, default: 1.5) \rightarrow 0	73.07	-0.24
Speech σ (ASR, default: 1.5) \rightarrow 4	72.51	-0.80
<i>Temporal decay factor κ (default: 2.0)</i>		
$\kappa=0.5$	72.83	-0.48
$\kappa=4.0$	72.67	-0.64
<i>Sigmoid sharpness γ (default: 3.0)</i>		
$\gamma=1.0$	73.07	-0.24
$\gamma=5.0$	72.99	-0.32

the neuro-symbolic architecture: frame relevance is determined by the compositional structure of the logic tree rather than by raw expert scores, so moderate changes to score processing have limited effect on the final frame ranking.

Smoothing bandwidths. Disabling smoothing entirely or zeroing visual smoothing leads to only a -0.08% drop. Over-smoothing (visual $\sigma=2$) causes a larger -1.04% drop by blurring shot boundaries. Speech smoothing shows a similar pattern: the default $\sigma_{\text{asr}}=1.5$ best bridges the coarser temporal resolution of transcripts, while both extremes degrade accuracy.

Temporal decay κ . Both a looser ($\kappa=0.5$, -0.48%) and tighter ($\kappa=4.0$, -0.64%) decay show that the RIGHTAFTER operator is effective across a range of decay rates.

Sigmoid sharpness γ . Reducing ($\gamma=1.0$) or increasing ($\gamma=5.0$) the sigmoid contrast both lead to drops under 0.33% , demonstrating that the median/MAD normalization is robust to the exact sharpness setting.

D.2 Expert Backbone Ablation

To evaluate whether HiMu’s gains depend on a specific set of pretrained models, we swap each expert’s underlying backbone one at a time (Table 7). All substitutions stay within $\approx 1\%$ of the default, with Grounding DINO even yielding a marginal improvement of $+0.40\%$. This confirms that HiMu’s strength lies in the hierarchical composition of multimodal signals rather than in any single expert backbone, allowing practitioners to substitute backbones based on deployment constraints with minimal accuracy degradation.

D.3 LLM Tree Parser Comparison

In the default configuration, Qwen3-VL-8B serves as both the tree parser and the downstream LVLM answerer; here we hold the answerer fixed and vary only the parser. We fix the downstream LVLM answerer (Qwen3-VL-8B) and vary only the LLM that generates the logic tree (Table 8). All

Table 7: Component-level ablation on a random 50% subset of Video-MME (Qwen3-VL-8B, $K=16$): expert backbone swaps and selection strategy. Each row changes one component from the default configuration. Δ is the difference from the baseline.

Configuration	Accuracy	Δ
HiMu (default)	73.31	—
<i>Expert backbone swap</i>		
CLIP-dfn [33] \rightarrow SigLIP2 [5]	72.59	-0.72
YOLO-World v2 [23] \rightarrow Grounding DINO [36]	73.71	+0.40
docTR [31] \rightarrow EasyOCR [37]	72.35	-0.96
faster-whisper large-v3-turbo [32] \rightarrow whisper-large [32]	72.67	-0.64
LAION CLAP [26] \rightarrow CLAP music-speech [26]	72.75	-0.56
<i>Selection strategy</i>		
PASS \rightarrow Vanilla top- K	72.59	-0.72

Table 8: Effect of LLM tree parser on Video-MME accuracy (50% subset, Qwen3-VL-8B as LVLMM answerer). Δ is the difference from the Qwen3-VL baseline.

Tree Parser LLM	Accuracy	Δ
Qwen3-VL-8B [1] (default)	73.31	—
LLaVA-OV-1.5-8B [38]	74.17	+0.86
Gemini-2.5-Flash [39]	73.31	0.00
InternVL-3.5-8B [40]	73.22	-0.09

four parsers—spanning open-source and proprietary models of different scales—achieve accuracy within a 0.95% range. This tight spread demonstrates that HiMu’s structured prompt and JSON schema constraint (Appendix A.2) effectively guide diverse LLMs toward trees that yield statistically equivalent selection accuracy on this benchmark, making the system robust to the choice of tree parser. Even the lowest-performing parser (InternVL-3.5-8B) achieves 73.22%, only 0.09% below the default.

Notably, the best-performing tree parser is LLaVA-OV-1.5-8B (+0.86%), despite being one of the weaker LVLMM *answerers* in our main experiments (Table 2 in the main paper): as a downstream answerer it reaches only 67.65% overall on Video-MME, well below Qwen3-VL-8B (73.22%), InternVL-3.5-8B (71.35%), and Gemini-2.5-Flash (76.11%). This decoupling between answering capacity and parsing effectiveness indicates that logic-tree generation is a structured decomposition task—governed by the prompt template and JSON schema—rather than an open-ended reasoning task that demands frontier-level language understanding. In practice, our results show that an open-source 8B model (LLaVA-OV-1.5-8B) can replace a large closed-source model (Gemini-2.5-Flash) as HiMu’s tree parser without any accuracy loss (+0.86% vs. 0.00%), indicating that HiMu’s selection stage does not require a frontier proprietary model when a capable open 8B parser is available.

E Selector Latency Breakdown

Table 1 in the main paper reports selector latency—excluding the final QA LLM call—for a 10-minute video sampled at 1 FPS (600 candidate frames, $K=16$) on $8\times A100$ (80 GB). **E2E** denotes the first-query latency including one-time preprocessing; **Amortized** denotes the per-query cost when video-level features have already been cached from a prior query on the same video. Table 9 breaks down HiMu’s selector latency into its constituent components.

Table 9: Per-component selector latency breakdown for HiMu on $8\times A100$ (80 GB). A 10-minute video at 1 FPS yields 600 candidate frames. Preprocessing is executed once per video and cached; per-query stages run for each new question. DP = data-parallel. †Conditional on the corresponding expert appearing in the logic tree; when absent, the component is skipped entirely.

Component	Hardware	Latency (s)
<i>Preprocessing (cacheable, one-time per video)</i>		
Video / audio I/O	CPU	1.3
CLIP-dfn ViT-L/14 (600 frames)	1 GPU	2.1
LAION CLAP (300 windows)†	1 GPU	0.9
docTR OCR (~300 frames)†	4 GPUs (DP)	3.0
faster-whisper lv3-turbo (10 min)†	3 GPUs	2.8
Preprocessing total (parallel)		4.3
<i>Per-query (amortized cost)</i>		
Query planning (8B parser)	1 GPU, CPU	6.7
OVD / YOLOv8x-worldv2 (600 frames)†	6 GPUs (DP)	2.1
Per-query scoring (text matching)	1 GPU	<0.2
Composition + PASS	CPU	<0.1
Per-query total		9.0
E2E total (preprocess + per-query)		13.3

Preprocessing. Video decoding and audio extraction (~1.3s on CPU) are followed by parallel expert feature extraction on 8 GPUs: CLIP frame embeddings and CLAP audio embeddings share GPU 0 (2.1 s + 0.9 s sequentially = 3.0 s), docTR runs on GPUs 1–4 (3.0 s), and Whisper transcription runs on GPUs 5–7 (2.8 s). The wall clock is determined by the slowest parallel branch: $1.3 + \max(3.0, 3.0, 2.8) = 4.3$ s. When no audio or text leaves appear in the tree, only CLIP features are needed and preprocessing drops to $1.3 + 2.1 = 3.4$ s.

Per-query processing. The amortized cost is dominated by the LLM tree parse (query planning) and open-vocabulary detection: OVD must re-run on all 600 frames for each new query because its text-conditioned detections depend on the OVD leaf queries produced by the logic tree. The reported 6.7 s term should be understood as the measured wall-clock cost of the query-planning stack on the chosen 8B parser implementation, including schema-constrained generation and tree materialization. OVD then executes sequentially after the tree is available, yielding a total per-query selector latency of 9.0 s. CLIP, OCR, ASR, and CLAP features are query-independent and reused directly from the cache; only a lightweight text-encoding and cosine-similarity lookup is required per query (<0.2s). Composition and PASS operate on 600-element score arrays via element-wise fuzzy-logic operations and peak detection, completing in under 100 ms on CPU.

Comparison with other method classes. Similarity-based selectors (BOLT, AKS, MDP³) achieve lower E2E latency (1.8–3.0s) by scoring frames with a single embedding pass, but lack compositional structure for multi-clause queries.¹ Structured methods (T*, VSLS) have comparable E2E (13.0–13.3s) yet cannot amortize: their query-conditioned detection loops re-execute entirely for every question, so amortized cost equals E2E. Multi-call methods (VideoAgent, SeViLA) are 3–5× slower due to iterative LLM calls within the selection loop. HiMu’s amortized bottleneck is the query-planning (~6.7s); accelerating that stage would directly reduce the per-query selector cost.

F Interpretability of Frame Selection

A key structural benefit of HiMu’s neuro-symbolic design is that every frame-selection decision is fully auditable. Because the satisfaction score $T(t)$ is computed by a deterministic fuzzy-logic tree over named leaf scores, each frame t carries an explicit attribution vector $\mathbf{a}(t) = (s_{e_1}^{(1)}(t), \dots, s_{e_L}^{(L)}(t)) \in [0, 1]^L$, where each entry records how strongly a specific expert-predicate pair fired at that frame. This stands in sharp contrast to similarity-based selectors (BOLT [6], AKS [7], MDP³ [8]), which collapse the entire question into a single embedding and return one opaque aggregate similarity scalar per frame, leaving no record of which part of the query drove selection or which modality was activated. Agent-based methods (VideoAgent [9], SeViLA [13]) produce readable reasoning steps but make frame-selection decisions implicitly, through opaque LLM outputs rather than an explicit scored ranking. Consequently, their outputs are difficult to inspect at the level of individual predicates: one cannot directly determine which predicate supported a selected frame, why two candidate frames were ranked differently, or whether a failure arose from perception, temporal composition, or query decomposition. In HiMu, by contrast, any selected frame can be immediately explained from its leaf activations—e.g., “this frame was chosen because the OVD leaf ‘*man in suit*’ scored 0.91 and the CLIP leaf ‘*applause*’ scored 0.83”—and any rejected frame can be confirmed to have scored uniformly low across all predicates.

Figure 7 illustrates this for a representative Video-MME question (“What does the black dog do in the water?”): each column is one of the $K=16$ selected frames; each row is a named leaf, coloured by its normalised score $s_e^{(i)}(t) \in [0, 1]$. The shared-context leaves under the root AND node—OVD: “black dog” and CLIP: “in water”—are uniformly dark across nearly all frames, confirming that the selected frames consistently depict the relevant scene. Within the OR over the four MCQ options, option-specific leaves exhibit clearly distinct activation patterns: for instance, CLIP: “submerging” fires strongly (1.00) on every frame, whereas CLIP: “searching” and OVD: “fish” are dark only in the earlier temporal cluster (~133–173s) and fade to pale in the later cluster (~459–586s), revealing which moments support which answer candidate. The bottom of the figure shows the corresponding frame thumbnails, letting a user visually verify the heatmap activations against the actual video content.

This interpretability has direct practical value: when HiMu answers a question incorrectly, the heatmap pinpoints whether the failure stems from a specific expert (e.g., OCR missing on-screen text), the tree structure (e.g., a SEQ operator with the wrong temporal ordering), or the query decomposition (e.g., an overly generic predicate). Such fine-grained, per-predicate transparency is, to our knowledge, unique among current frame-selection methods and turns HiMu into a diagnostic tool—not merely a preprocessing step—that enables practitioners to iteratively refine expert configurations, tree templates, and smoothing parameters with targeted, evidence-based feedback.

¹Latency figures for BOLT, AKS, MDP³, T*, and VSLS are estimated from their respective published reports, adjusted to an 8×A100 (80 GB) reference; we did not re-measure these baselines.

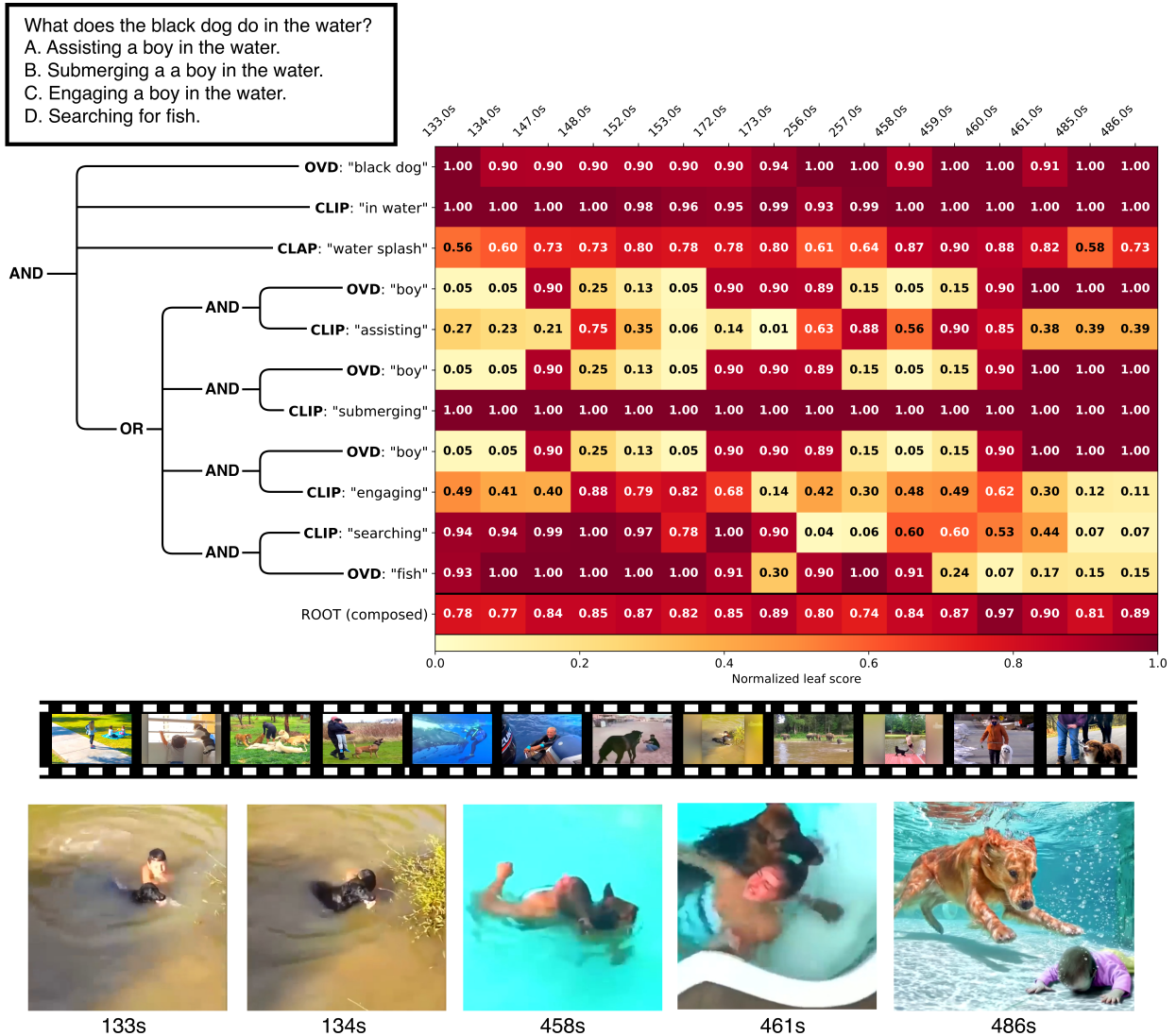


Figure 7: **Per-leaf activation heatmap for a sampled Video-MME question.** *Top-left*: the MCQ question (“What does the black dog do in the water?”) with its four answer options. *Centre*: the logic tree with per-leaf scores for each of the $K=16$ selected frames (columns, in temporal order). Cell colour encodes $s_e^{(i)}(t) \in [0, 1]$ (dark ≈ 1 : predicate strongly satisfied; light/pale ≈ 0 : not satisfied). *Bottom*: a filmstrip of few of the 1 fps sampled frames and enlarged thumbnails of five representatives from the selected frames. This leaf-level transparency is a structural consequence of HiMu’s neuro-symbolic design and is unavailable in similarity-based or agent-based selectors.